Opto-Electronics Review

Dual tracking of MPP for PV under diffuse irradiation and urban microclimatic conditions using sub-interval prediction via Bayesian-optimized regression

Jenifer Suriya L. J.[1*], Christy Mano Raj J. S.[2]

[1] Loyola-ICAM College of Engineering and Technology, Chennai 600034, India

[2] Government College of Engineering, Bargur 635104, India

Article info	Abstract
	Optimal power extraction from a photovoltaic (PV) plant in urban and rural areas varies due to microclimatic conditions and diffuse irradiations. Traditional methods such as Perturb and Observe (P&O) and Incremental Conductance (INC) are used in urban and rural PV power plants. Diffuse irradiation and microclimatic conditions are different in urban and rural areas. Moreover, one of two sides of the PV characteristics is used for tracking the maximum power point (MPP), i.e., either constant voltage or constant current region. In this paper, a Bayesian-optimized multiple regression-based dual tracking (BM-DT) is proposed for a sub-intervals prediction technique (SIPT) and the tracking of MPP is done using both sides of the PV characteristics. Moreover, the voltage step used for tracking the MPP is not a fixed quantity and is predicted using BM. The proposed BM-DT technique predicts sub-intervals from a specified initial voltage interval. Moreover, the maximum power point is tracked through interval and SIPT, based on microclimatic conditions. As tracking is done along both sides of the photovoltaics (PV), the performance with outstanding power extraction efficiencies at low, medium, and high power levels is 99%, 99.2% and 99.4%, respectively.

1. Introduction

Optimization methods are used in maximum power point tracking (MPPT) for maximum power extraction. MPPT algorithms are selected based on the pattern of irradiation on all photovoltaic (PV) cells/modules, such as uniform irradiation and non-uniform irradiation. Uniform irradiation leads to more power delivery from the PV modules rather than non-uniform irradiation.

Many techniques were proposed for MPPT under uniform and non-uniform irradiated conditions. Most of the techniques implemented in MPPT are for uniform irradiation, with a control algorithm that is less complex and faster in convergence. MPPT techniques used for non-uniform irradiation conditions are complex in nature and require an effective control technique for convergence.

Another categorization of the MPPT methods for PV modules are off-line and online methods. In the online

method, the PV module operating parameters, such as module terminal voltage (V_{pv}) and current (I_{pv}), are regularly measured and processed through the control algorithm. The control algorithm tracks the maximum power point (MPP) continuously, increasing the efficiency of the PV system.

The traditional on-line methods, such as Perturb and Observe (P&O) and Incremental Conductance (INC) methods, are used in the MPPT. Many new methods have been developed to improve MPPT performance by adjusting control parameters. Modified P&O and INC methods focus on step size, where the step sizes are modified with respect to dP/dV [1], dP/dI [2], dI/dD [3], dP/dD [4] in the entire range of control space. Based on the above parameters, the adaptation is tuned empirically and hence loses generalization [2].

In specific modified P&O methods, the PV curve is divided into several sectors/regions and the step sizes are

*Corresponding author at: jenifersuriya.lj@licet.ac.in

modified based on the voltage sector/region on the PV curve in which the operating point lies [5–6], and in another similar variant, the step size is modified based on the distance of the operating point from the MPP [7]. Another modified P&O method incorporates a momentum term to the step size, where selecting a momentum factor was crucial for faster tracking [8]. In [9], the P&O method is based on multi-sampling of the neighbourhood, which determines the direction of tracking on the PV curve under varying irradiation to avoid incorrect tracking.

In a few variants, the step size is modified only around the MPP at a steady state [10–11] and reduces the oscillations in MPP. Few methods change the PV parameters, such as PV voltage, power, and current and determine the perturbation size for the next iteration, enhancing the tracking performance during varying irradiation conditions [12–14]. Optimization-based MPPT methods track MPP for an optimal operating point based on the parameters of the PV module [15–19]. Existing MPPT methods are complex and need many PV parameters leading to high computational costs.

Different intelligent techniques are used in MPPT-based intelligent control methods, each with several stages of implementing a specific module [20–24].

In [25], an MPPT controller has a boundary controller using a second-order switching surface in the inner control loop and tracks the reference voltage generated by the dP/dV tracker in the outer loop. This dP/dV tracker tracks the PV characteristics using samples of two consecutive points along the constant voltage or the constant current region. Furthermore, the switching instants of the switch in the converter depend on the geometry of the input capacitor voltage and current, leading to a varying switching frequency under transient periods.

Nowadays, integrated building PV with more efficient PV modules using good transparent conductive oxide have become popular [26], where installations in urban regions require low reflectance value by using texturized glasses, which ultimately reduces the electric power output by around 5% [27]. Hence, under such circumstances, MPPT is essential to extract the remaining available power without much loss

1.1. Research questions (RQ)

1.1.1 (RQ1) Do the microclimatic conditions influence solar irradiations, and how can the MPP be implemented for maximum power extraction?

An attempt has been made to develop a new method for the MPPT technique which has less complexity and computational burden but has fast tracking and generalization by invoking voltage intervals and then making them converge towards the MPP under uniform irradiation conditions. Such a conceived method, Bayesian-optimized multiple regression-based dual tracking (BM-DT) is presented in this paper. The proposed sub-interval predicting technique (SIPT) method, also presented in this paper, consists of BM-DT that predicts the voltage interval along with microclimatic data which are used to fix the new intervals in such a way as to reach the MPP without divergence.

1.1.2 (RQ2) How to improve the MPP during the diffuse irradiation (DI) which occurs in the urban area and extract maximum power from a PV array?

The proposed BM-DT method tracks the MPP along both sides of the PV characteristics, one along the constant current (CC) region and the other along the constant voltage (CV) region towards the MPP. These two tracking processes follow one after the other in the convergence process. The BM-DT is proposed for SIPT. The BM-DT method presented in this paper uses the module general data, microclimatic data of panel planted such as urban/rural areas, and also periodically measures the module terminal voltage and current to implement the control algorithm to track the MPP effectively along with urban/rural microclimatic data. The module data are required with microclimatic data to implement the presented algorithm, which are the open circuit voltage V_{oc} and the MPP voltage V_{mpp} both at a standard test condition (STC) and can be easily obtained from the specification sheet provided by the manufacturer. No special efforts are required to obtain the same and the microclimatic data are included in the MPP, which is obtained from weather monitoring sensors.

2. I-V and PV characteristics of a PV module

Characteristics of a PV module are non-linear due to the presence of a PN junction in every PV cell. The generation of a PV current is linearly dependent on the level of irradiation. The non-linear mathematical model of a PV module current vs. voltage characteristics is represented in (1) [28]. The corresponding single-diode electrical equivalent circuit model of a PV module is shown in Fig. 1.

$$I_{pv} = I_p - I_{os}\left\{\exp\left(\frac{V_{pv} + I_{pv}N_s R_{se}}{n N_s V_T}\right) - 1\right\} - \left(\frac{V_{pv} + I_{pv}N_s R_{se}}{N_s R_{sh}}\right), \quad (1)$$

where V_{pv} is the PV module output voltage, I_{pv} is the PV module output current, I_p is the photocurrent produced due to irradiation, I_{os} is the reverse saturation current, V_T is the thermal voltage, N_s represents the number of cells in series, R_{sh} is the shunt resistance, R_{se} is the series resistance and the ideality factor of the PV cell.
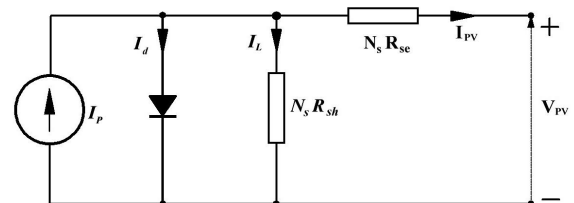

Fig. 1. Single-diode electrical equivalent circuit model of a PV module.

As the adaptation time of the proposed method is shorter compared to changing environmental parameters such as module temperature, location humidity, and wind speed impact, a simple model of the PV modules is considered.

A graphical representation of the I-V characteristics is shown in Fig. 2, which was obtained by solving (1) numerically through the Newton-Raphson method for

different uniform irradiation levels. Similarly, the PV characteristics of the PV module shall be obtained numerically and plotted in Fig. 3 for different uniform irradiation levels. It is obvious from Fig. 2 and Fig. 3 that both the *I-V* and PV characteristics are non-linear, and the PV characteristics exhibit unique points at which the power delivered through the PV module is at the maximum, and such points are known as MPPs.
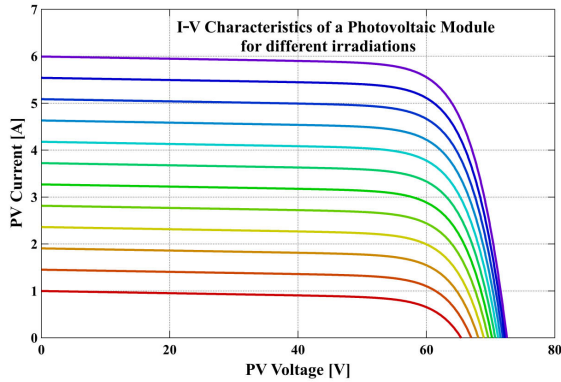

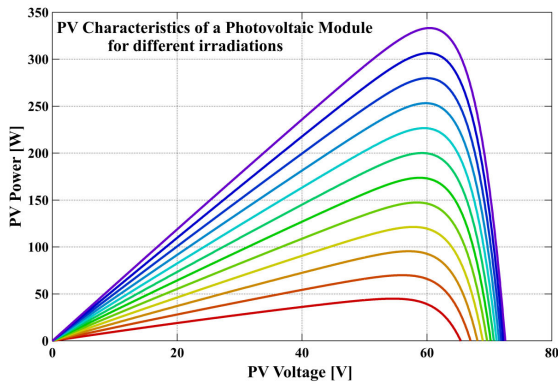**Fig. 2**. *I-V* characteristics of a PV module for different irradiations.

Fig. 3. P-V characteristics of a PV module for different irradiations.

To extract maximum power from the PV module under the prevailing environmental condition, a power electronic converter circuit is interposed between the PV module and the load. The converter is operated using control techniques and different algorithms.

3. Dual tracking sub-interval predicting technique (SIPT) of MPP

The proposed SIPT method presented in this paper consists of BM-DT, which predicts the voltage interval along with microclimatic data, which is used to fix the new intervals in such a way as to reach the MPP without divergence. The method is graphically illustrated in Fig. 4.

3.1. Bayesian-optimized multiple regression for dual tracking (BM-DT)

Bayesian optimization automates the search for optimal hyperparameters in regression models, which is often a resource-intensive process. Bayesian optimization uses the Gaussian process and predicts the performance of different
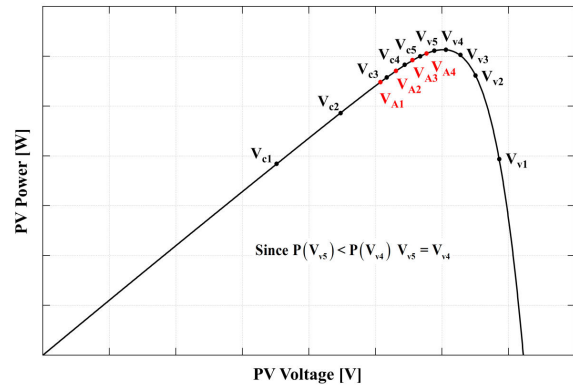

Fig. 4. Concept of a dual tracking sub-interval prediction technique (SIPT) of MPPT with microclimatic data.

hyperparameter combinations based on previous evaluations. This method focuses on the hyperparameter space leading to better results due to lower mean squared error, adaptability, and uncertainty management.

Bayesian optimization provides a natural framework for quantifying uncertainty in predictions. It captures the inherent variability in data and model predictions by generating posterior distributions for model parameters rather than point estimates. This capability allows practitioners to construct credible intervals around predictions, offering insights into their reliability. The advantages of BM-DT are robustness to outliers, model flexibility, and improved model selection.

Bayesian optimization facilitates model comparison by calculating posterior probabilities for different models. This capability enables practitioners to select models based on performance while taking into account uncertainty and prior beliefs about model effectiveness. Bayesian optimization helps identify which model best explains the data while considering uncertainty in parameter estimates.

Recent advancements in Bayesian linear regression allow for scalable approaches that maintain efficiency even as data size increases, making them suitable for small datasets. Bayesian optimization enhances multiple regression models by streamlining hyperparameter tuning, effectively managing uncertainty, and facilitating robust model selection. This leads to improved predictive accuracy and reliability in various applications across data science and machine learning domains.

 # Pseudocode for Bayesian-optimized multiple regression (BM-DT)

```
# Step 1: Define the model
  function BayesianRegressionModel(X, y):
    # X: Input features
    # y: Target variable
    # Define prior distributions for weights
      and bias
    w_prior = Normal(0, 1) # Prior for weights
    b_prior = Normal(0, 1) # Prior for bias
# Step 2: Define the likelihood function
    function likelihood(X, y, w, b):
    predictions = X * w + b
    return Normal(predictions, sigma)
  # Assuming normally distributed errors
# Step 3: Set up the Bayesian optimization
 process
    Function Bayesian Optimization (objective_
    function, bounds):
```

```
    # Initialize Gaussian Process model
      gp_model = GaussianProcess()
# Step 4: Randomly sample initial points from
  the bounds
      initial_samples=RandomSample(bounds,num_
      samples)
  # Evaluate the objective function at initial
    points for sample in initial_samples:
      y_sample = objective_function(sample)
      gp_model.update(sample, y_sample)
# Step 5: Iteratively optimize
      for iteration in range(max_iterations):
  # Update the Gaussian Process model with new
    observations
      gp_model.update()
# Step 6: Find the next point to evaluate using
  acquisition function
      next_point=maximize_acquisition_function (gp_
      model)
      # Evaluate the objective function at the new
        point
      y_next = objective_function(next_point)
      gp_model.update(next_point, y_next)
# Step 7: Define the objective function for
  regression
    function objective_function(params):
    X_train,y_train =load_data()
    # Load training data
    model=BayesianRegressionModel(X_train,y_train
)
  # Fit model with current parameters and return
    a metric (e.g., MSE)
      return compute_mse(model)
  # Main execution flow
    bounds = define_bounds()
  # Define parameter bounds for optimization
BayesianOptimization(objective_function, bounds)
```

An initial voltage interval is fixed based on the PV module open circuit voltage V_{oc} and the maximum power point voltage V_{mpp} at STC given in the specification sheet by the manufacturer. One of the voltage interval points is on the CC region, which is fixed between 0 V and the V_{mpp}, preferably greater than the mean of 0 V and the V_{mpp}, i.e., $V_{mpp}/2$. The other voltage interval point is on the CV region which is fixed at or around the mean of the V_{mpp} and the open circuit voltage V_{oc}, i.e., $(V_{mpp} + V_{oc})/2$.

After fixing the initial voltage interval points, the DC-DC converter is operated so that the PV modules operate at the predetermined voltage interval points, called V_{c0} and V_{v0}, one by one, and the respective output power delivered by the PV modules, i.e., $P(V_{c0})$ and $P(V_{v0})$, is measured.

In the first iteration, the initial voltage interval points are predicted with BM-DT, as in (2). Where α and β are constant, H represents the humidity in %, T represents the temperature of the area in °C and W represents the wind speed in mph where the PV array is installed.

$$Y\left(V_{A0} - Predicted\right) = \alpha\left(V_{c0}\right) + \beta_1\left(V_{v0}\right) + \beta_2\left(W\right) + \beta_3\left(T\right) + \beta_4\left(H\right). \quad (2)$$

With the computed voltage V_{A0}, the initial voltage interval is sub-divided into two sub-intervals such as $[V_{c0}, V_{A0}]$ and $[V_{A0}, V_{v0}]$. Then, the new values of voltage interval points are predicted from the sub-intervals using the BM-DT, which are given by the following equations:

$$Y\left(V_{c1} - Predicted\right) = \alpha\left(V_{c0}\right) + \beta_1\left(V_{A0}\right) + \beta_2\left(W\right) + \beta_3\left(T\right) + \beta_4\left(H\right), \quad (3)$$

$$Y\left(V_{v1} - Predicted\right) = \alpha\left(V_{v0}\right) + \beta_1\left(V_{A0}\right) + \beta_2\left(W\right) + \beta_3\left(T\right) + \beta_4\left(H\right). \quad (4)$$

The PV modules are again made to work at these new voltage interval points and the respective power delivered by the PV modules at these new voltage interval points aremeasured as $P(V_{c1})$ and $P(V_{v1})$.

The same procedure is followed in the second iteration; however, before retaining the voltage interval points V_{c1} and V_{v1} for the next interval computation, a power check needs to be performed, as stated below.

If $P(V_{c1}) > P(V_{c0})$, V_{c1} is retained otherwise $V_{c1} = V_{c0}$, similarly if $P(V_{v1}) > P(V_{v0})$, V_{v1} is retained otherwise $V_{v1} = V_{v0}$. Upon evaluation of the above criteria, the second prediction is computed and these procedures are repeated until a predetermined tolerance is satisfied for both the power and the voltage interval points. It is clear that the prediction optimization continues until the voltage interval shrinks and eventually converges to a single point or closer to each other when a predetermined tolerance for voltage interval is satisfied, where the power delivered by the PV modules will be at the maximum or very close to the maximum power which depends on the tolerance.

In general, the interval average and the sub-interval average, which are the voltage interval points for the next iteration, are predicted as per the following expressions:

$$Y\left(V_{An} - Predicted\right) = \alpha\left(V_{cn}\right) + \beta_1\left(V_{vn}\right) + \beta_2\left(W\right) + \beta_3\left(T\right) + \beta_4\left(H\right), \quad (5)$$

$$Y\left(V_{cn+1} - Predicted\right) = \alpha\left(V_{cn}\right) + \beta_1\left(V_{An}\right) + \beta_2\left(W\right) + \beta_3\left(T\right) + \beta_4\left(H\right), (6)$$

$$Y\left(V_{vn+1} - Predicted\right) = \alpha\left(V_{vn}\right) + \beta_1\left(V_{An}\right) + \beta_2\left(W\right) + \beta_3\left(T\right) + \beta_4\left(H\right). \quad (7)$$

In the SIPT method of MPPT, at every iteration, both sides of the voltage interval are adjusted and the adjustment of the voltage interval is based on the prediction of the sub-intervals created by the average of the interval.

3.2. General procedure of the proposed technique of MPPT

1. Set iteration number 'n' to 0. Give initial values to the voltage interval as V_{c0} and V_{v0} and drive the converter to operate at these voltages consecutively.
2. Obtain the powers $P(V_{c0})$, $P(V_{v0})$ at V_{c0} and V_{v0}, respectively.
3. Predict the values of V_{c0} and V_{v0} as given by (2).
4. Increase 'n' and determine the new voltage interval values given by the following expressions:

$$Y\left(V_{cn+1} - Predicted\right) = \alpha\left(V_{cn}\right) + \beta_1\left(V_{An}\right) + \beta_2\left(W\right) + \beta_3\left(T\right) + \beta_4\left(H\right), \quad (8)$$

$$Y\left(V_{vn+1} - Predicted\right) = \alpha\left(V_{vn}\right) + \beta_1\left(V_{An}\right) + \beta_2\left(W\right) + \beta_3\left(T\right) + \beta_4\left(H\right). (9)$$

5. Apply new voltage values to the converter.
6. Obtain new powers $P(V_{cn+1})$ and $P(V_{vn+1})$.
7. Check if $P(V_{cn+1})$ is greater/less than $P(V_{cn})$ and $P(V_{vn+1})$ is greater/less than $P(V_{vn})$.
8. If $P(V_{cn+1})$ is greater than $P(V_{cn})$, V_{cn+1} shall be carried over to next iteration. Otherwise, reject V_{cn+1} and make $V_{cn+1} = V_{cn}$.
9. If $P(V_{vn+1})$ is greater than $P(V_{vn})$, V_{vn+1} shall be carried over to next iteration. Otherwise, reject V_{vn+1}, make $V_{vn+1} = V_{vn}$.

10. Compute the interval average and the sub-interval prediction for the next iteration using the following expressions:

$$Y\left(V_{An+1} - Predicted\right) = \alpha\left(V_{cn+1}\right) + \beta_1\left(V_{vn+1}\right) + \beta_2\left(W\right) + \beta_3\left(T\right) + \beta_4\left(H\right),$$ (10)

$$Y\left(V_{cn+2} - Predicted\right) = \alpha\left(V_{cn+1}\right) + \beta_1\left(V_{An+1}\right) + \beta_2\left(W\right) + \beta_3\left(T\right) + \beta_4\left(H\right),$$ (11)

$$Y\left(V_{vn+2} - Predicted\right) = \alpha\left(V_{vn+1}\right) + \beta_1\left(V_{An+1}\right) + \beta_2\left(W\right) + \beta_3\left(T\right) + \beta_4\left(H\right).$$ (12)

11. Find the change in power and voltage as given in (13) and (14):

$$\left|\Delta P\right| = P\left(V_{cn+1}\right) - P\left(V_{vn+1}\right),$$ (13)

$$\Delta V = V_{cn+1} - V_{vn+1}.$$ (14)

12. Check whether ΔP and ΔV are less than tolerance.
13. If either ΔP or ΔV violates the tolerance, increase 'n' and go to step 5; otherwise, go to step 14.
14. Stop changing the voltage intervals.
15. Apply perturbation to the final value of either V_c or V_v for 'N' times to check for any change in irradiation during iteration.
16. Check whether the power increases and exceeds a predetermined threshold value.
17. If the power is increasing and greater than the predetermined threshold value, proceed to step 1; otherwise, proceed to step 18.
18. Continuously check for any change in irradiation level. If not, repeat step 18; otherwise go to step 1.

3.3. Simulation of SIPT using BM-DT

The proposed SIPT method for MPPT is verified through computer simulations. The computer simulations are carried out with the help of a PLECS software. In the simulations:

i) start-up behaviour, ii) dynamic behaviour when a change in irradiation takes place before reaching a steady state, and iii) dynamic behaviour when a change in irradiation takes place after reaching a steady state of the SIPT method are studied using BM-DT.

The schematic used for the SIPT method of MPPT is illustrated in Fig. 5. The intended application of the complete circuit is to charge batteries. A PV array, consisting of two strings comprising three numbers of PV modules all connected in series, is connected to two 12 V batteries, connected in series through a buck converter. The simulation study is configured with the intention of determining the behaviour of PV power, voltage, current, and their convergence when the SIPT method is deployed. In all the cases, to visualize the convergence of the SIPT method, illustrations are made by superimposing the time variation of PV voltage and power to create power *vs.* voltage trace. Furthermore, this research is meant for uniform irradiation conditions and although the temperature of the environment and module takes into account the self-heating phenomenon, it is not explicitly considered.

3.4. Start-up behaviour in microclimatic conditions

The start-up behaviour of the system is considered a vital performance index as it shows, under non-uniform irradiation, how fast the MPP is reached and its convergence pattern. The start-up performance of the proposed SIPT method is studied under the following environmental parameters: i) irradiation – 600 W/m^2, (ii) temperature – 25 °C and microclimatic conditions such as i) land surface temperature – 25 °C, ii) humidity, and iii) wind speed at nominal values of the considered location (Chennai and Tiruvallur urban areas) as specified in section 5. During tracking, the movement and the convergence of the interval points and their corresponding powers are illustrated in Fig. 6. The net convergence behaviour of the SIPT method during start-up is illustrated in Fig. 7. From Fig. 6 and Fig. 7, SIPT tracking performance and its convergence towards the MPP are appealing. The time variation of PV power, voltage, and current are illustrated in Fig. 8.
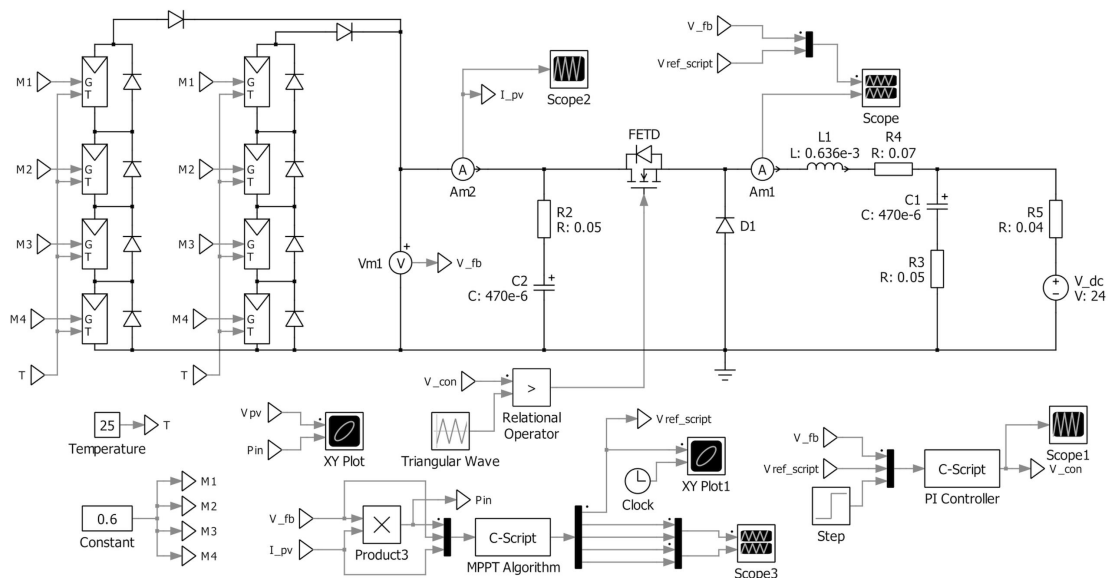

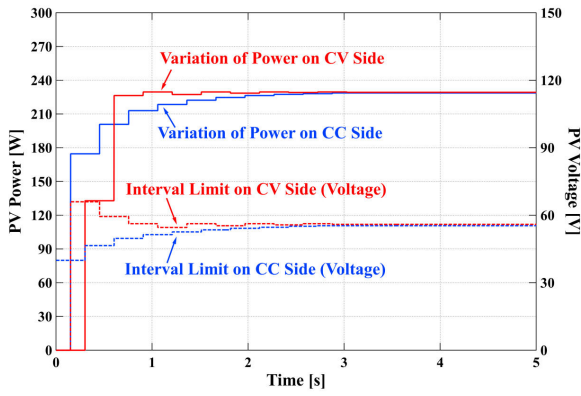**Fig. 5.** Scheme for verification of the SIPT method by computer simulation.

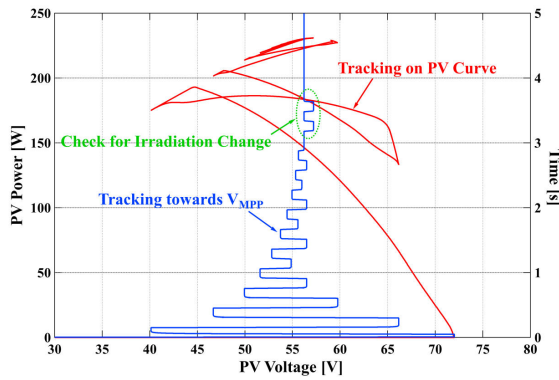**Fig. 6.** Convergence of interval points of SIPT.

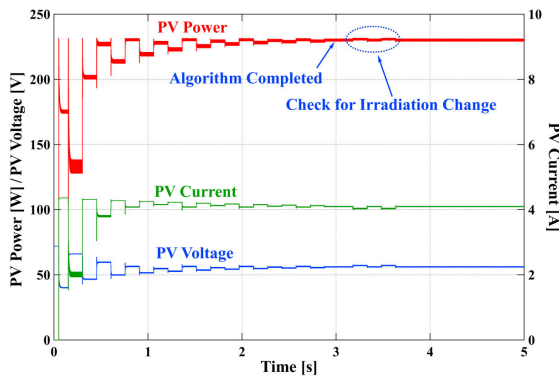**Fig. 7.** Net convergence of SIPT during start-up.

Fig. 8. Time variation of PV power, voltage, and current at start-up.

From the simulation, after reaching a steady state, the power extracted from the PV array by the SIPT method is 230.21 W and the true maximum power, which is the peak power at a particular environmental condition, is 231.12 W.

3.5. Dynamic behaviour due to daily insolation (DI) is changed before reaching steady state

Dynamic behaviour was studied and the convergence performance was assessed under varying environmental microclimatic parameters such as (i) wind speed, (ii) humidity, and (iii) surface land temperature. The dynamic behaviour of the SIPT method is studied with the following environmental parameters: i) initial irradiation – 600 W/m^2 at start-up, ii) initial irradiation – 200 W/m^2, and final irradiation – 800 W/m^2, where the change was initiated before reaching steady state, iii) initial irradiation –

500 W/m^2 and final irradiation – 900 W/m^2, where the change was initiated after reaching steady state, iv) temperature – 25 °C and nominal microclimatic parameters such as v) wind speed, vi) humidity, vii) surface land temperature. The change in the irradiation magnitude had been applied before SIPT and reached its steady state. The convergence behaviour and the time behaviour of PV parameters are illustrated in Fig. 9 and Fig. 10. In this case of dynamic behaviour, the final power extracted from the PV array after reaching the steady state is 315.46 W and a true maximum power is 318.1 W.
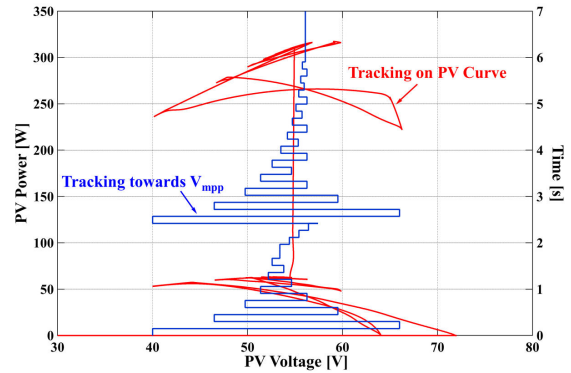

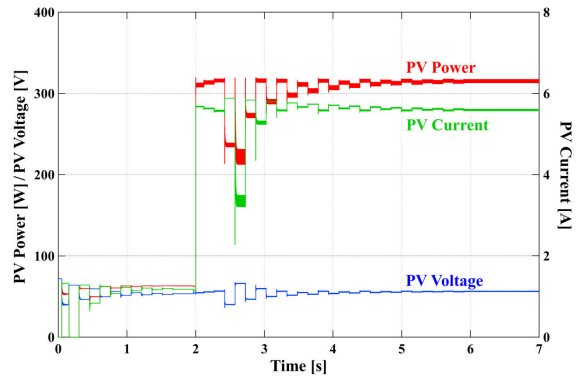**Fig. 9.** Tracking/convergence behaviour of SIPT when irradiation is changed before steady state.

Fig. 10. Time variation of PV power, voltage, and current when irradiation is changed before steady state.

3.6. Dynamic behaviour of DI is changed after reaching steady state

Performance characteristics of the SIPT method were investigated, when the magnitude of DI is changed after reaching steady state, and the behaviours are illustrated in Fig. 11 and Fig. 12 for convergence and combined time variation of power, voltage, and current, respectively.

A simulation study for this condition gives the final power extracted from the PV array after reaching steady state as 360.69 W and the true maximum power is 361.98 W.

4. The experimental bedtest of SIPT and BM-DT in different urban and rural locations

The bedtest is used to validate the SIPT method of MPPT and confirm the results obtained in the simulations. The experimental setup consists of: i) PV array consisting of four modules of 125 W$_p$ each with ($V_{oc} = 21.8$ V, $V_{mpp} = 17.4$ V) connected in series, ii) buck converter,
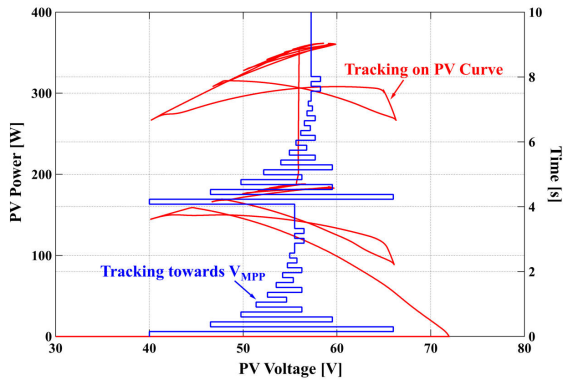
Fig. 11. Tracking/convergence behaviour of SIPT when irradiation is changed after steady state.
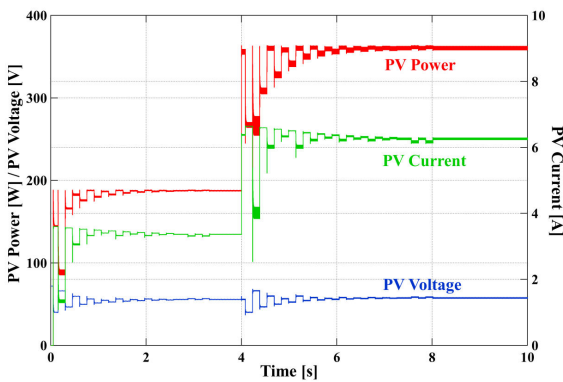

Fig. 12. Time variation of PV power, voltage, and current when irradiation is changed after steady state.

iii) three 12 V batteries of 100 Ah capacity connected in series, and iv) control circuit configured around dsPIC30F2010. The values of the passive components used in the buck converter in the experimental testbed are the same as those of the values used in the simulation studies.

The following equipment take measurements: i) Keysight DSO DSOX3014T to monitor dynamics of the SIPT method, ii) Tektronix DSO TPS2024 to capture the PV parameters, and iii) MECO Solar Array Analyzer to find the true maximum power from the PV array. The experimental setup is shown in Fig. 13.

In the experimental study, an iteration step size fixed in the software is 400 msec producing better clarity in the illustrations. The start-up performance of the SIPT method is experimentally verified under a low power-level, medium-power level, and at a high-power level. Experimentally obtained results are shown in Fig. 14 to Fig. 16. The extracted power from the PV array under the above-mentioned power levels is 104 W, 360 W, and 488 W,
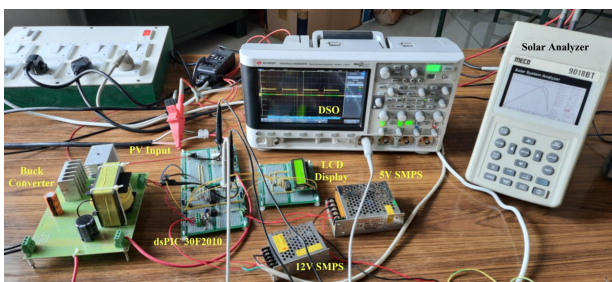

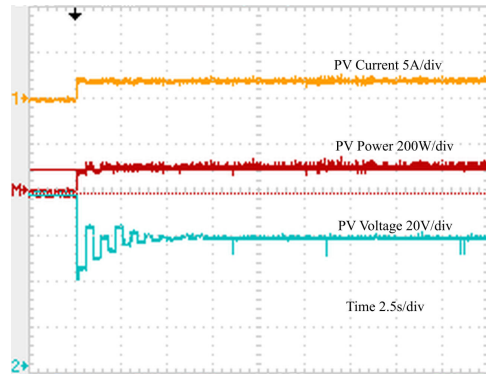**Fig. 13.** Experimental set-up to verify the SIPT method.

Fig. 14. Start-up behaviour of SIPT at low-power level.
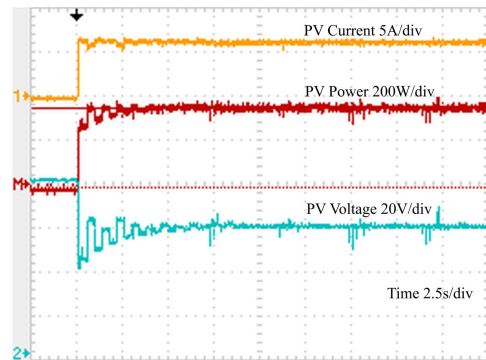

Fig. 15. Start-up behaviour of SIPT at medium-power level.
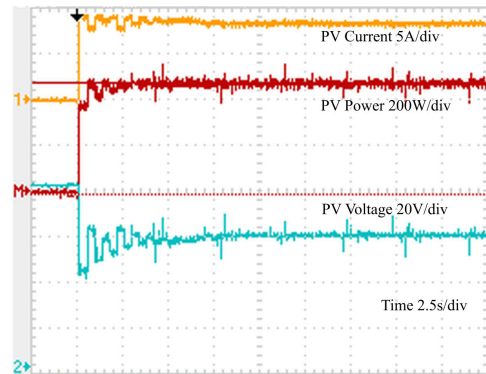

Fig. 16. Start-up behaviour of SIPT at high-power level.

respectively, against the true maximum powers, which is the maximum power (peak power at a particular environmental condition) measured by a solar array analyser of 105 W, 363 W, and 491.6 W, as measured through the Solar Array Analyzer. The typical graphical illustration of the tracking and convergence performance of the SIPT method under medium-power level is obtained by superimposing the time variation in PV voltage towards the MPP on the power-voltage trace obtained from the data captured by a digital storage oscilloscope (DSO), as shown in Fig. 17, which gives an excellent correlation with the simulated results.

The performance of the SIPT method is verified under dynamic variation of DI during natural cloud movements and different microclimatic conditions. The tracking performance under such dynamic environmental conditions is shown in Fig. 18. This illustration shows the excellent behaviour of the SIPT method in tracking and convergence towards MPP.

The speed of the tracking process depends on the proper design of the PI controller and its effect on the settling time of the PV array voltage to the set reference voltage given by the SIPT method. The settling time of the designed PI controller implemented with a 30F2010 dsPIC digital signal controller is 30 ms. Setting the iteration time period to 30 ms improves the tracking speed and the convergence time of the proposed method is measured at 660 ms. The converging performance with this iteration time period is captured using a digital storage oscilloscope and illustrated in Fig. 19.

5.   Results and discussion

The proposed SIPT method with BM-DT prediction is introduced in this paper and has an excellent tracking performance and power extraction efficiency. This is obvious
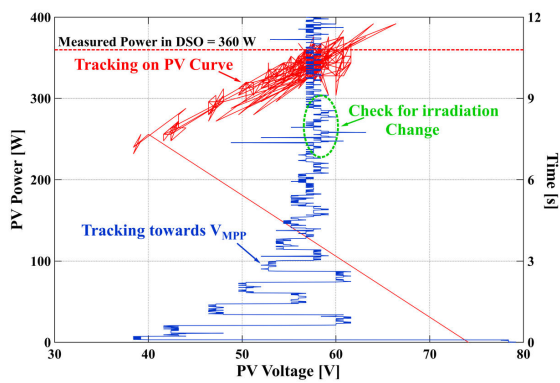

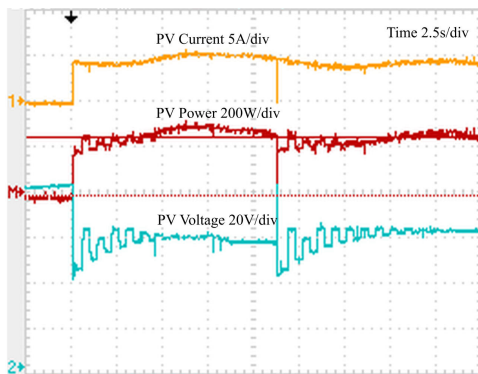**Fig. 17.** Convergence behaviour of SIPT at medium-power level.

Fig. 18. Dynamic behaviour of SIPT under natural variation of irradiation.
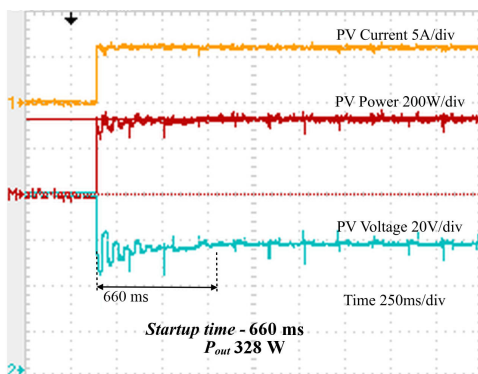

Fig. 19. Illustration of convergence time with an iteration time of 30 ms.

from the simulation study which is performed under three different situations as presented in section 4; the power extraction efficiencies are calculated as 99.6%, 99.1%, and 99.6%, with an excellent tracking performance. This has clearly shown the SIPT method success with BM-DT prediction in MPPT. The tracking process precisely follows the algorithm used to implement the SIPT method.

The experimental verification of the SIPT method showed a testimony to its performance and exhibited an excellent correlation with the simulation results. The experimental study made at three different power output levels has produced a well-acceptable tracking performance with outstanding power extraction efficiencies at low, medium, and high-power levels as 99%, 99.2%, and 99.4%, respectively. The accuracy of the measured results is well within $\pm 2\%$ of the absolute readings. In addition, the tracking speed of the SIPT method under DI and urban microclimatic conditions of MPP is shown as 660 ms with the dsPIC30F2010 digital signal controller. Furthermore, tracking convergence is well-established under naturally varying DI and urban microclimatic conditions without any divergence. Altogether, the overall performance of the SIPT method of MPPT is shown through simulation and experimental results and leads to this proposed method being an excellent method for PV array applications with uniform irradiation.

5.1. DI in urban areas and solar panels

DI refers to solar radiation that reaches the Earth's surface after being scattered by atmospheric particles, clouds, and other obstructions. This type of radiation is crucial for solar energy applications, particularly in urban environments where buildings can obstruct direct sunlight. DI is very high in urban areas. Urban areas typically experience different patterns of DI compared to rural settings due to factors such as building density, pollution, and atmospheric conditions. For instance, studies have shown that cities like Chennai in Tamil Nadu, India receive varying amounts of DI depending on the season and local atmospheric conditions. On clear days, Chennai areas receive up to 15.6% more DI in June than nearby rural areas like Tiruvallur in Tamil Nadu. The presence of particulate matter and urban heat can enhance scattering, thus increasing the diffuse component of solar radiation. The impact on solar panel performance during MPP is higher. Figure 20 shows the DI due to high buildings near solar panels.

Solar panels can use direct and diffuse solar radiation, making them effective even in less-than-ideal conditions. The amount of DI influences the performance of PV systems. DI is the sunlight that reaches the panels directly
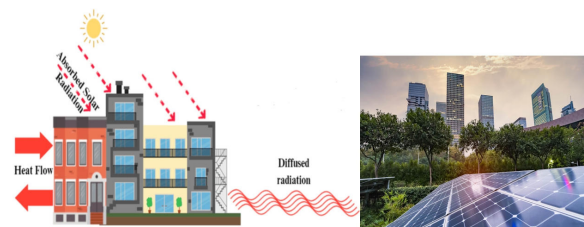

Fig. 20. DI due to high buildings near solar panels.

from the Sun. It is most effective when panels are oriented towards the Sun. DI is critical during times when clouds obscure direct sunlight. Due to this diffused light, PV systems can still generate electricity under overcast conditions. This study indicates that urban environments can significantly affect the DI available to solar panels. For example, a study highlighted the importance of modelling DI on tilted surfaces in urban settings, considering factors like building orientation and surrounding structures. Tables 1 and 2 show the DI and predicted outpower of the proposed BM-DT algorithm for Chennai urban area and Tiruvallur rural area, respectively, where DI represents the daily insolation, H represents the humidity in %, T represents the temperature of the area in °C, and W represents the wind speed in mph, P_{out} and P_{in} represent the output and input power in watts, and η is the efficiency in %. Figure 21 shows (a) a histogram of residuals, (b) a standard probability plot of residuals for the Chennai urban area, and Figure 22 shows the same for the Tiruvallur rural area. histogram allows analysts to inspect whether the residuals are approximately normally distributed visually. This is crucial because many statistical tests and confidence intervals rely on the assumption of normality in residuals.

This study used accuracy, specificity, and sensitivity in solar testing. Sensitivity (true positive rate) measures the proportion of actual positives that are correctly identified by the test.

$$Sensitivity = [TP]/[TP + FN], \qquad (15)$$

where TP equals true positives (correctly identified positive cases) and FN = false negatives (actual positives incorrectly identified as negative).

Specificity (true negative rate) measures the proportion of actual negatives that are correctly identified by the test.

$$Specificity = [TN]/[TN + FP], \qquad (16)$$

where TN = true negatives (correctly identified negative cases) and FP = false positives (actual negatives incorrectly identified as positive).

Accuracy measures the overall correctness of the test, indicating the proportion of true results (both positives and negatives) among the total number of the cases examined.
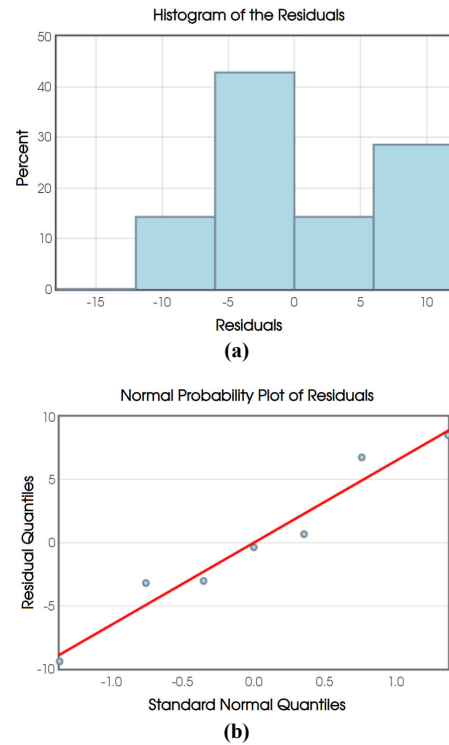
$$Accuracy = [TP + TN]/[TN + FP + FN]. \qquad (17)$$

(a)

(b)

Fig. 21. (a) Histogram of residuals, (b) normal probability plot of residuals for Chennai urban area.

Table 1.
DI and predicted outpower of the proposed BM-DT algorithm (Chennai urban area).

Date and time Day – D; Evening – E	DI (MJ/m²/day)	T (°C)	H (%)	W (mph)	P_{out} (W) Actual	P_{out} (W) Predicted	η (%)
7/6/24 (D)	18.67	29	84	8	388	387	99.74
9/7/24 (E)	19.25	32	75	9	400	398	99.50
8/8/24 (D)	21.97	28	82	8	360	358	99.44
15/9/24 (D)	24.36	31	86	7	350	348	99.42
16/9/24 (D)	22.45	32	87	6	412	411	99.75
20/9/24 (E)	23.45	36	74	8	436	435	99.77
21/9/24 (E)	18.32	37	84	8	399	387	96.99

Table. 2.
DI and predicted outpower of the proposed BM-DT algorithm (Tiruvallur rural area).

Date and time Day – D; Evening – E	DI (MJ/m²/day)	T (°C)	H (%)	W (mph)	P_{out} (W) Actual	P_{out} (W) Predicted	η (%)
17/5/24(D)	15.32	28	90	9	350	346	98.86
18/6/24(E)	14.32	26	84	10	345	342	99.13
25/8/24(D)	13.25	25	86	9	354	352	99.43
26/9/24(D)	12.36	24	89	11	356	350	98.31
2/9/24 (D)	14.25	25	85	10	400	398	99.50
22/9/24(E)	17.39	26	80	12	412	411	99.75
29/9/24(E)	16.27	27	81	10	425	421	99.05

(a)

(b)
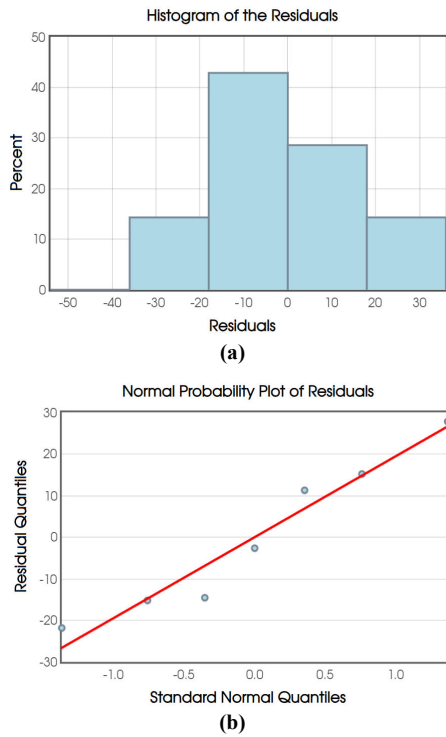
Fig. 22. (a) Histogram of residuals, (b) normal probability plot of residuals for Tiruvallur rural area.

Fig. 23. Accuracy and specificity for the proposed BM-DT (Chennai urban area).

Fig. 24. Accuracy and specificity for the proposed BM-DT (Tiruvallur rural area).

Figure 23 compares the performance metrics such as accuracy, sensitivity, and specificity of the proposed Bayesian-optimized decision tree model with the two benchmark methods presented in [29] and [30] at Chennai urban area, whereas Figure 24 does the same for Tiruvallur rural area. The diffuse horizontal irradiance is measured with a pyranometer shaded by a shadow ball.

5.2. Discussion

MPPT algorithms are used for optimizing the energy output of PV systems during different environmental conditions. The output characteristics of PV cells are nonlinear and vary with different irradiance levels. As DI increases, the overall power output of the PV system is changed and affects the location of the MPP on the voltage-current (*V-I*) curve. Under conditions of a high DI, MPP shifts and requires MPPT algorithms to adapt quickly to maintain optimal performance. When MPPT algorithm is slow to respond, it may not effectively capture the maximum available power, which leads to reduced efficiency.

In summary, DI plays a critical role in determining the efficiency of MPPT systems in PV applications. The ability of the MPPT algorithm to adapt to changing irradiance conditions, especially those involving significant diffuse radiation, has greatly influenced the overall energy production. Proper sensor calibration and choice of MPPT technique are essential for optimizing performance under varying atmospheric conditions. The presence of DI alters the power output characteristics of PV panels. As diffuse radiation increases, the PV system voltage-current (*V-I*) curve changes, shifting the MPP upwards. MPPT algorithms must continuously adapt to these changes to optimize energy capture effectively.

The distribution of residuals obtained from the Bayesian-optimized regression model presented in histogram in
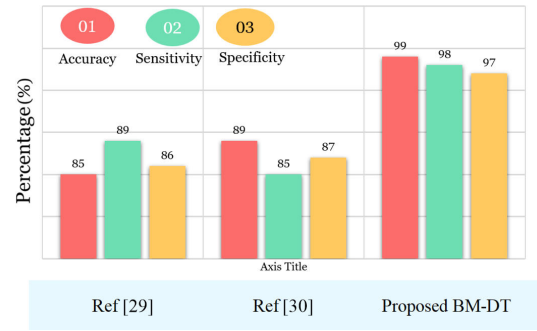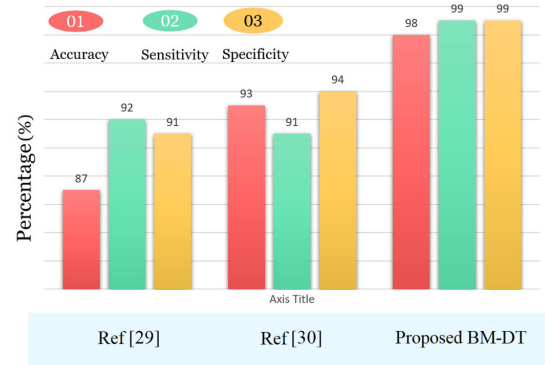
Figs. 21(a) and 22(a) is divided into bins to group residuals, showcasing their distribution. A majority of the residuals are concentrated near the zero-residual value, indicating a low average deviation between predicted and actual values, which reflects the accuracy of the Bayesian-optimized regression in estimating the MPP. The histogram indicates the effectiveness of the optimization technique. The concentration of residuals around zero suggests that the model minimizes prediction errors, making it suitable for the applications. The histogram also validates the model effectiveness in minimizing errors for power output predictions under varying solar conditions.

Examining normality over a wider range of residuals captures extreme cases where predictions significantly deviate in the form of normal probability plot to assess the normality of residuals from the regression model in Figs. 21(b) and 22(b). These figures demonstrate the model sensitivity to unusual solar or environmental conditions. All the residuals were closely aligned with the diagonal line, indicating that the model errors are approximately normally distributed and that the proposed Bayesian regression model is robust. The normality of residuals is crucial for ensuring the reliability of the Bayesian optimization in tracking the true MPP.

Further from the charts in Figs. 23 and 24, corresponding to two different locations, the performance of the proposed method of MPPT has outperformed the other two techniques mentioned in [29] and [30] with respect to the accuracy of tracking and sensitivity to environmental parameters, and specificity in tracking to reach the MPP under uniform irradiation without any divergence. These qualities underscore the proposed BM-DT model reliability and robustness in adapting to the

nonlinear characteristics of solar MPPT systems and substantiate their reliability and effectiveness in optimized power extraction form PV modules.

DI notably influences the efficiency of MPPT algorithms due to its impact on the power output characteristics of PV systems. Algorithms that can quickly adapt to changes in diffuse radiation, such as INC, tend to perform better than those that do not adjust as dynamically, such as P&O. Understanding these dynamics is essential for optimizing energy production, especially in environments with variable cloud cover and diffuse light conditions. The proposed BM-DT algorithm performs the adaptation within 660 ms on average based on microclimatic conditions parameters, whereas P&O method adaptation time is 990 ms on average with microclimatic data.

6. Conclusions

A new method to track the MPP by sub-interval prediction using the BM-DT method for a PV array under DI and different urban microclimatic conditions is presented in this paper. The proposed SIPT method is verified through software simulations. These simulations have confirmed its validity regarding attaining the MPP with greater accuracy and convergence. Experimental verifications were carried out to confirm the validity of the proposed SIPT and BM-DT methods. It is shown that there was an excellent congruence between the results obtained through simulations and experimental work. Moreover, it has been shown that the time taken by the proposed method has an MPP of 660 ms using a low-cost digital signal controller. The performance of the presented method with changes in ID and urban microclimatic condition levels is excellent with appealing convergence; in addition, the efficiency in power extraction with different ID levels and urban microclimatic conditions is more than 99%.

Moreover, due to an excellent estimation of MPP and the proposed technique good reliability and robustness, the user can extract optimal power from PV modules with very good efficiency. Further, as the adaptation time is very short without any divergence in tracking compared with other techniques, the user can obtain a very good overall efficiency in power extraction using the proposed BM-DT method. Finally, as the system is configured around a low-cost digital signal controller with less complexity and computation, the overall cost of the MPP tracker using the proposed technique is lower and affordable to any user.

Authors' statement

Research concept and design, collection and/or assembly of data, data analysis and interpretation, writing the article, Jenifer Suriya L.J. and Christy Mano Raj J.S.; critical revision of the article, Jenifer Suriya L.J.; final approval of article, Christy Mano Raj J.S.

References

[1] Pandey, A., Dasgupta, N. & Mukerjee, A. K. Design Issues in Implementing MPPT for Improved Tracking and Dynamic Performance. in *IECON 2006 – 32nd Annual Conference on IEEE Industrial Electronics* 4387–4391 (IEEE, 2006). https://doi.org/10.1109/IECON.2006.348008

[2] Mei, Q., Shan, M., Liu, L. & Guerrero, J. M. A novel improved variable step-size incremental-resistance MPPT method for PV systems. *IEEE Trans. Ind. Electron.* **58**, 2427–2434 (2011). https://doi.org/10.1109/TIE.2010.2064275

[3] Jiang, Y., Abu Qahouq, J. A. & Haskew, T. A. Adaptive step size with adaptive-perturbation-frequency digital MPPT controller for a single-sensor photovoltaic solar system. *IEEE Trans. Power Electron.* **28**, 3195–3205 (2013). https://doi.org/10.1109/TPEL.2012.2220158

[4] Femia, N., Petrone, G., Spagnuolo, G. & Vitelli, M. Optimization of perturb and observe maximum power point tracking method. *IEEE Trans. Power Electron.* **20**, 963–973 (2005). https://doi.org/10.1109/TPEL.2005.850975

[5] Swaminathan, N., Lakshminarasamma, N. & Cao, Y. A fixed zone perturb and observe MPPT technique for a standalone distributed PV system. *IEEE J. Emerg. Sel. Topics Power Electron.* **10**, 361–374 (2022). https://doi.org/10.1109/JESTPE.2021.3065916

[6] Ali, A. I. M. Sayed, M. A. & Mohamed, E. E. M. Modified efficient perturb and observe maximum power point tracking technique for grid-tied PV system. *Int. J. Electr. Power Energy Syst.* **99**, 192–202 (2018). https://doi.org/10.1016/j.ijepes.2017.12.029

[7] Necaibia, S., Kelaiaia, M. S., Labar, H., Necaibia, A. & Castronuovo, E. D. Enhanced auto-scaling incremental conductance MPPT method, implemented on low-cost microcontroller and SEPIC converter. *Sol. Energy* **180**, 152–168 (2019). https://doi.org/10.1016/j.solener.2019.01.028

[8] Raiker, G. A., Loganathan, U. & Subba Reddy, B. Current control of boost converter for PV interface with momentum-based perturb and observe MPPT. *IEEE Trans. Ind. Appl.* **57**, 4071–4079 (IEEE, 2021). https://doi.org/10.1109/TIA.2021.3081519

[9] Abouadane, H., Fakkar, A., Sera, D., Lashab, A., Spataru, S. & Kerekes, T. Multiple-power-sample based P&O MPPT for fast-changing irradiance conditions for a simple implementation. *IEEE J. Photovolt.* **10**, 1481–1488 (IEEE, 2020). https://doi.org/10.1109/JPHOTOV.2020.3009781

[10] Ahmed, J. & Salam, Z. An improved perturb and observe (P&O) maximum power point tracking (MPPT) algorithm for higher efficiency. *Appl. Energy* **150**, 97–108, 2015. https://doi.org/10.1016/j.apenergy.2015.04.006

[11] Başoğlu, M. E. An enhanced scanning-based MPPT approach for DMPPT systems. *Int. J. Electron.* **105**, 2066–2081 (2018). https://doi.org/10.1080/00207217.2018.1494332

[12] Belkaid, A., Colak, I. & Isik, O. Photovoltaic maximum power point tracking under fast varying of solar radiation. *Appl. Energy* **179**, 523–530 (2016). https://doi.org/10.1016/j.apenergy.2016.07.034

[13] Pathak, P. K., Padmanaban, S., Yadav, A. K., Alvi, P. A. & Khan, B. Modified incremental conductance MPPT algorithm for SPV-based grid-tied and stand-alone systems. *IET Gener. Transm. Distrib.* **16**, 776–791 (2022). https://doi.org/10.1049/gtd2.12328

[14] Devi, V. K., Premkumar, K., Bisharathu Beevi, A. & Ramaiyer, S. A modified Perturb & Observe MPPT technique to tackle steady state and rapidly varying atmospheric conditions. *Sol. Energy* **157**, 419–426 (2017). https://doi.org/10.1016/j.solener.2017.08.059

[15] Zadeh, M. J. Z. & Fathi, S. H. A new approach for photovoltaic arrays modelling and maximum power point estimation in real operating conditions. *IEEE Trans. Ind. Electron.* **64**, 9334–9343 (2017). https://doi.org/10.1109/TIE.2017.2711571

[16] Ahmed, M., Abdelrahem, M., Harbi, I. & Kennel, R. An adaptive model-based MPPT technique with drift-avoidance for grid-connected PV systems. *Energies* **13**, 6656–6680 (2020). https://doi.org/10.3390/en13246656

[17] Li, Q. *et al*. An improved perturbation and observation maximum power point tracking algorithm based on a PV module four-parameter model for higher efficiency. *Appl. Energy* **195**, 523–537 (2017). https://doi.org/10.1016/j.apenergy.2017.03.062

[18] Peng, L., Zheng, S., Chai, X. & Li, L. A novel tangent error maximum power point tracking algorithm for photovoltaic system under fast multi-changing solar irradiances. *Appl. Energy* **210**, 303–316 (2018). https://doi.org/10.1016/j.apenergy.2017.11.017

[19] Li, S., Ping, A., Liu, Y., Ma, X. & Li, C. A variable-weather-parameter MPPT method based on a defined characteristic resistance of photovoltaic cell. *Sol. Energy* **199**, 673–684 (2020). https://doi.org/10.1016/j.solener.2020.02.065

[20] Yap, K. Y., Sarimuthu, C. R. & Lim, J. M.-Y. Artificial intelligence based MPPT techniques for solar power system: A review. *J. Mod. Power Syst. Clean Energy* **8**, 1043–1059 (2020). https://doi.org/10.35833/MPCE.2020.000159

[21] Kermadi, M. & Berkouk, E. M. Artificial intelligence-based maximum power point tracking controllers for photovoltaic systems: Comparative study. *Renew. Sustain. Energy Rev.* **69**, 369–386 (2017). https://doi.org/10.1016/j.rser.2016.11.125

[22] Çelik, Ö. & Teke, A. A hybrid MPPT method for grid connected photovoltaic systems under rapidly changing atmospheric conditions. *Electr. Power Syst. Res.* **152**, 194–210 (2017). https://doi.org/10.1016/j.epsr.2017.07.011

[23] Tang, S. *et al.* An enhanced MPPT method combining fractional-order and fuzzy logic control. *IEEE J. Photovolt.* **7**, 640–650 (2017). https://doi.org/10.1109/JPHOTOV.2017.2649600

[24] Bataineh, K. Improved hybrid algorithms-based MPPT algorithm for PV system operating under severe weather conditions. *IET Power Electron.* **12**, 703–711 (2019). https://doi.org/10.1049/iet-pel.2018.5651

[25] Zhou, Y., Ho, C. N. M. & Siu, K. K.-M. A fast PV MPPT scheme using boundary control with second-order switching surface. *IEEE J. Photovolt.* **9**, 849–857 (2019). https://doi.org/10.1109/JPHOTOV.2019.2899470

[26] Kwaśnicki, P. *et al.* Characterization of the TCO layer on a glass surface for PV IInd and IIIrd generation applications. *Energies* **17**, 3122 (2024). https://doi.org/10.3390/en17133122

[27] Kwaśnicki, P. Texturized glass in the application of architectural photovoltaics. *Clean. Eng. Technol.* **22**, 100810 (2024). https://doi.org/10.1016/j.clet.2024.100810

[28] Christy Mano Raj, J. S. & Jeyakumar, A. E. A two stage successive estimation based maximum power point tracking technique for photovoltaic modules. *Sol. Energy* **103**, 43–61 (2014). https://doi.org/10.1016/j.solener.2014.01.042

[29] Padmavathi, N., Chilambuchelvan, A. & Shanker, N. R. Maximum power point tracking during partial shading effect in PV system using machine learning regression controller. *J. Electr. Eng. Technol.* **16**, 737–748 (2021). https://doi.org/10.1007/s42835-020-00621-4

[30] Ishrat, Z., Gupta, A. K. & Nayak, S. A comprehensive review of MPPT techniques based on ML applicable for maximum power in solar power systems. *J. Renew. Energy Environ.* **11**, 28–37 (2024). https://doi.org/10.30501/jree.2023.385661.1556